Study of mixed ionic-electronic conduction mechanism in perovskite oxides using Rietveld refinements and the maximum-entropy method analysis of *in situ* synchrotron X-ray diffraction data

Recently, mixed ionic–electronic conductivity (MIEC) in perovskite oxides $ABO_{3-\delta}$ (A indicates an alkaline and/or rare earth metal, while B represents a transition metal) has generated great interest in the development of electrochemical devices such as cathodes for solid oxide fuel cells (SOFCs), oxygen pumps, oxygen sensors, catalysts, and oxygen separation membranes. In particular, SOFCs, which can directly convert chemical energy to electricity, have increasingly attracted worldwide attention owing to their outstanding characteristics such as high efficiency and significantly low emission levels of pollutants. However, an important technical concern present in SOFCs needs to be overcome, namely, the operation temperature of the cells. The operation temperature needs to be reduced to 750–1000 K. To solve this issue, it is indispensable to understand the MIEC mechanism of SOFC cathode materials in detail (Fig. 1). Shao *et al.* have presented $(Ba_{0.5}Sr_{0.5})(Co_{0.8}Fe_{0.2})O_{3-\delta}$ (BSCF) as a promising cathode material for next-generation SOFCs [1]. Extensive studies of BSCF have been conducted on the electrochemical properties, oxygen nonstoichiometry, and crystal structure of perovskite oxides. However, they do not explain why the electrochemical properties of BSCF make it more suited for use in low-temperature-operated SOFCs than other cathode materials.

The maximum-entropy method (MEM) analysis for calculating charge density from X-ray data is a promising approach for studying the bonding state, atomic disorder, and ion conduction in detail [2].

We undertake to discuss the MIEC mechanism in cathode materials of SOFCs by using Rietveld refinements and MEM analysis of *in situ* synchrotron X-ray diffraction (SR-XRD) measurements at 500–900 K for the first time, and compare the temperature dependence of the charge density of

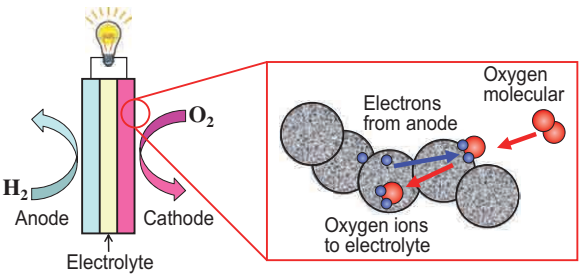

Fig. 1. Role of cathode material in SOFCs.

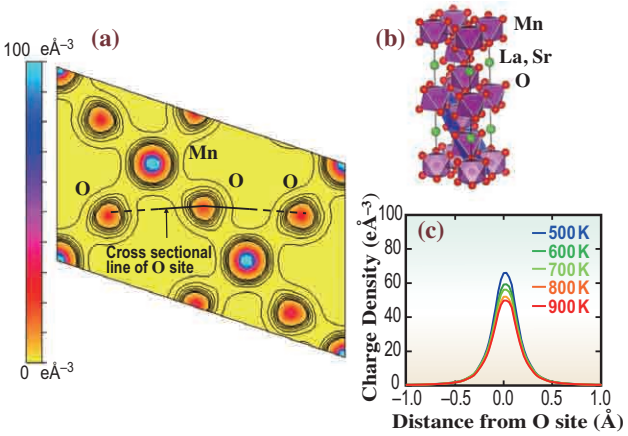

Fig. 2. **(a)** Charge density distribution at 500 K for $R\bar{3}c$ Mn-O ($\bar{1}02$) plane of LSM, contour line: 0-5 eÅ^{-3}, step: 0.6 eÅ^{-3}. **(b)** Crystal structure for $R\bar{3}c$ Mn-O ($\bar{1}02$) plane of LSM. **(c)** One-dimensional charge density profile around the O site at 500-900 K for $R\bar{3}c$ along the line in the direction to another O site in the Mn-O plane.

$(La_{0.75}Sr_{0.25})MnO_{3-\delta}$ (LSM, SOFC cathode material operating at high temperature) with that of BSCF (SOFC cathode material operating at low temperature). SR-XRD experiments were carried out using a large Debye-Scherre camera installed at **BL19B2**. The Rietveld refinement used the program RIETAN–FP [3] and the MEM analysis used the program PRIMA. The crystal structures and the charge density were visualized using the software package VESTA [4], which is based on VENUS software.

Figure 2(a) shows the charge density distribution of the Mn–O ($\bar{1}02$) plane at 500 K. This plane possesses isotropic Mn–O bonds, and these bonds show strong covalency in LSM. This result supports the fact that LSM has high electron conductivity. For a strong covalent bond of Mn–O, oxygen ions would be prevented from participating in conduction. In fact, the oxygen ion conductivity of LSM is lower than that of other perovskite oxides that are used as cathode materials for an SOFC. Figure 2(c) shows the one-dimensional charge density profiles around an O site along the line to another O site on the Mn–O plane at 500–900 K. The charge density profiles decrease slightly with an increase in temperature. We speculate that this phenomenon is related to the increase in the atomic isotropic displacement parameter (U_{iso}) and not to the decrease in oxygen site occupancy.

Figure 3(a) shows the charge density distribution (202) plane of BSCF at 500 K. In Fig. 3(b), the red-colored part of the oxygen site indicates the oxygen site occupancy. We found that the anisotropic bonds in the (Co, Fe)–O1(4*c*) and O2(8*d*) planes in BSCF, and the O1(4*c*) site possess more vacancies than the O2(8*d*) site. The (Co, Fe)–O1(4*c*) bond was less covalent than the (Co, Fe)–O2(8*d*) bond in BSCF. Figures 3(c) and 3(d) show the one-dimensional charge density profile around the O1(4*c*) site along the line to the O2(8*d*) site and the O2(8*d*) sites along the line to the O1(4*c*) site at 500–900 K, respectively. The charge density profiles of the O2(8*d*) site were independent of temperature. It can be speculated that the O2(8*d*) site occupancy does not change with an increase in temperature. On the other hand, the charge density profiles of the O1(4*c*) site dramatically decreased with an increase in temperature. We inferred that the charge density profile expanded to another oxygen site for oxygen ion conduction. The (Co, Fe)–O2(8*d*) plane is involved in conducting electrons for the strong-covalency bond and has a low concentration of oxygen vacancies. In contrast, the (Co, Fe)–O1(4*c*) plane with a high concentration of oxygen vacancies and ionic bonds would be involved in the diffusion of oxygen ions. We understand that the BSCF structure has covalent and ionic bonds; this is different from the case of LSM, which has only strong covalent bonds. We assume that the presence of covalent and ionic bonds is more effective for MIEC in SOFCs operating at low temperatures than the presence of single-type bond suchs as the Mn–O bond in LSM.

Finally, we point out the attention of MEM analysis. MEM analysis possesses several issues in high-temperature diffraction measurement. In particularly, the current MEM analysis does not take account of thermal diffuse scattering (TDS) which increases with an increase in temperature. Therefore, there is a possibility that TDS reduces the accuracy of the charge density at high temperature estimated by MEM analysis. We hope that the consideration of TDS is incorporated into Rietveld refinements and MEM analysis. MEM analysis, however, is very useful and indispensable in discussing the charge density and MIEC mechanism in the crystal structure.

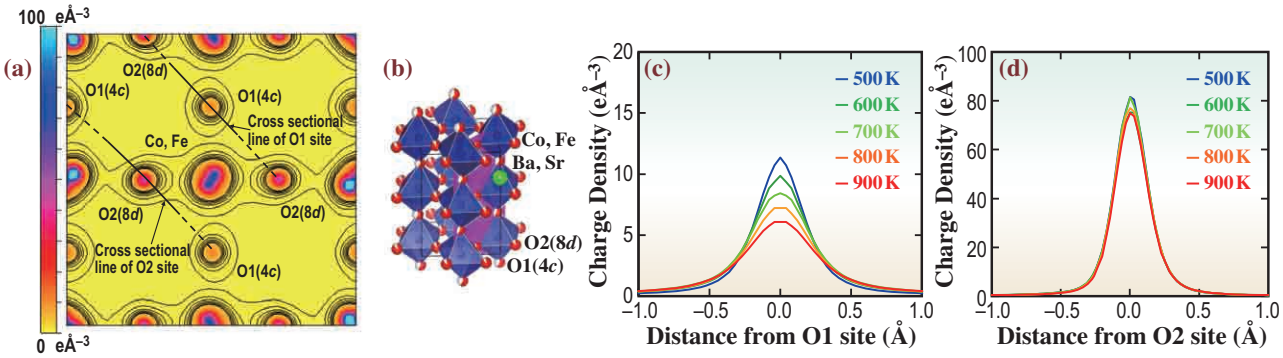

Fig. 3. **(a)** Charge density distribution at 500 K for *Pnma*, (Co, Fe)-O1, O2 (202) plane of BSCF, contour line: 0-5 eÅ^{-3}, step: 0.6 eÅ^{-3}. **(b)** Crystal structure for *Pnma*, (Co, Fe)-O1, O2 (202) plane of BSCF. **(c)** One-dimensional charge density profile around the O1 site at 500-900 K for *Pnma* along the line in the direction to another O2 site in the (Co, Fe)-O2 plane. **(d)** One-dimensional charge density profile around the O2 site at 500–900 K for *Pnma* along the line in the direction to another O1 site in the (Ba, Sr)-O1 plane.

Takanori Itoh[a,*], Keiichi Osaka[b] and Ichiro Hirosawa[b]

[a] AGCSeimichemical Co., Ltd.
[b] SPring-8/JASRI

*E-mail: tknitoh@seimichemical.co.jp

References

[1] Z. Shao and S.H. Haile: Nature **431** (2004) 170.
[2] M. Sakata and M. Sato: Acta Crystallogr. A **46** (1990) 263.
[3] F. Izumi and K. Momma: Solid State Phenom. **130** (2007) 15.
[4] K. Momma and F. Izumi: J. Appl. Crystallogr. **44** (2011) 1272.
[5] *T. Itoh, S. Shirasaki, Y. Fujie, N. Kitamura, Y. Idemoto, K. Osaka, H. Ofuchi, S. Hirayama, T. Honma and I. Hirosawa: J. Alloys Comp.* ***491*** *(2010) 527.*